RELATING WORLDVIEW-2 DATA TO PINE PLANTATION LIDAR METRICS

J.C. Trinder [a], A. Shamsoddini [a, b, *], R. Turner [c]

[a] School of Civil and Environmental Engineering, University of New South Wales, Sydney, Australia - (j.trinder, a.shamsoddini)@unsw.edu.au
[b] Department of Remote Sensing & GIS, Tarbiat Modares University, Tehran, Iran
[c] Remote Census, Sydney, Australia - remote.census@outlook.com

KEY WORDS: Lidar, Optical, Spectral, Texture, Prediction, Forestry

ABSTRACT:

Over last decades, different types of remotely sensed data including lidar, radar and optical data were investigated for forest studies. Undoubtedly, lidar data is one of the promising tools for these purposes; however, the accessibility and cost of this data are the main limitations. In order to overcome these limitations, optical data have been considered for modelling lidar metrics and their use for inferring lidar metrics over areas with no lidar coverage. WorldView-2 (WV-2) data as a high resolution optical data offer 8 bands including four traditional bands, blue, green, red, and infrared, and four new bands including coastal blue, yellow, red edge and a new infrared band whose relationships with lidar metrics were investigated in this study. For this purpose, band reflectance, band ratios, and principal components (PCs) of WV-2 multispectral data along with 23 vegetation indices were extracted. Moreover, the grey level co-occurrence matrix (GLCM) indices of bands, band ratios and PCs were also calculated for different window sizes and orientations. Spectral derivatives and textural attributes of WV-2 were provided for a stepwise multiple-linear regression to model 10 lidar metrics including maximum, mean, variance, 10^{th}, 30^{th}, 60^{th} and 90^{th} height percentiles, standard error of mean, kurtosis and skewness for a *Pinus radiata* plantation, in NSW, Australia. The results indicated that the textural-based models are significantly more efficient than spectral-based models for predicting lidar metrics. Moreover, the integration of spectral derivatives with textural attributes cannot improve the results derived from textural-based models. The study demonstrates that WV-2 data are efficient for predicting lidar metrics.

1. INTRODUCTION

Conventional forestry methods such as field sampling and direct surveying which sometimes involve destructive techniques (Jinha and Crawford, 2012) are constrained by time and cost (Hyyppä et al., 2000). Also, the extrapolation of the results of these methods to a large forest is likely to be erroneous (Chen et al., 2011). Moreover, accessibility of some forest areas is a critical issue that would significantly increase costs of surveys (Shanmugam et al., 2006). Considering these difficulties, earth observation technologies have been exploited as an economic source of data for extracting more current and accurate structural parameters at global to local scales than can be achievable by *in situ* methods (Le Toan et al., 2004). Among different types of remotely sensed data, discrete lidar data has been used to estimate and calculate different structural parameters including tree height (Popescu et al., 2002; Dean et al., 2009), biomass and biomass-related variables such as stand volume, and basal area (Means et al., 1999; Smart et al., 2012; Shamsoddini et al., 2013b). Lidar data can provide a direct measure of tree or stand height (Hyde et al., 2006; Erdody and Moskal, 2010) and is arguably superior in this regard compared to other remote sensing options. Lidar-derived tree height is useful for predicting other forest parameters such as stand volume, but factors such as canopy closure and density must also be considered (Lim et al., 2003).

However, significant constraints on applying lidar data are the high data acquisition cost (Lefsky et al., 2001), which varies as a function of factors such as pulse density, topography and project location, especially at regional scales, (Sexton et al., 2009; Chen and Hay, 2011); limited existing coverage (Hyyppä et al., 2008); and the computations which are required to process these data (Donoghue and Watt, 2006). For these reasons, the prediction of lidar metrics using other remotely sensed data, especially optical data such as Landsat TM and ETM+, and QuickBird data, has been recently proposed and a limited number of studies have been conducted for this purpose (Wulder and Seemann, 2003; Hilker et al., 2008; Chen and Hay, 2011). Different types of information, including spectral derivatives and textural information were extracted from optical data by various researchers to relate them to the lidar metrics (Chen and Hay, 2011). More investigations are require on which types of data are most useful for prediction of lidar metrics. Also, it should be determined whether the addition of spectral derivatives to the textural data can improve the results of lidar metric prediction. The launch of new optical satellites such as WorldView-2 (WV-2) offering simultaneously new spectral bands and high resolution data calls for the investigation of the capabilities of these new data and spectral bands for predicting lidar metrics. Among different types of lidar metrics, the prediction of lidar-derived mean and maximum canopy heights has been investigated more frequent than the others using multiple-linear regression as a common modelling method (Hilker et al., 2008; Pascual et al., 2010); However, the other lidar-derived height metrics, such as variance (Zimble et al., 2003), skewness, and percentiles of

* Corresponding author

lidar-derived heights (Shamsoddini et al., 2013b), are also useful for estimating forest structural parameters.

According to the above considerations, this paper aims to:

- Investigate the utility of WV-2 data for predicting different lidar metrics.
- Compare the performances of the textural-based and spectral-based models derived from WV-2 for lidar metric prediction.
- Investigate the effect of spectral information on the improvement of the accuracy of lidar metric prediction derived from textural indices alone.

In the next sections, the study area and remotely sensed data used for this study are explained. Then, the methodology and results are given and finally the results are discussed and conclusions are presented.

2. STUDY AREA AND DATA

2.1 Study Area

The study area shown in figure 1 includes a 5000 ha *Pinus radiata* plantation, from 35° 23′ 35″ S to 35° 29′ 58″ S latitude, and 147° 58′ 48″ E to 148° 04′ 02″ E longitude, within a larger 20,400 ha commercial estate in the vicinity of Batlow in the Hume region of Forests, NSW, Australia. The pine plantation includes a variation of terrain conditions, tree ages and thinning conditions. While 62% of the plantation covers the areas with the slope of 0° to 10°, the slope classes of 10° to 20° and more than 20° dominate 35% and 3% of the plantation, respectively. Also, unthinned, first thinning and second thinning classes cover 52%, 25%, and 23% of the plantation, respectively. Moreover, while 47% of the area is dominated by the trees of 10 to 20 years old, 53% of the trees are older than 20 years.

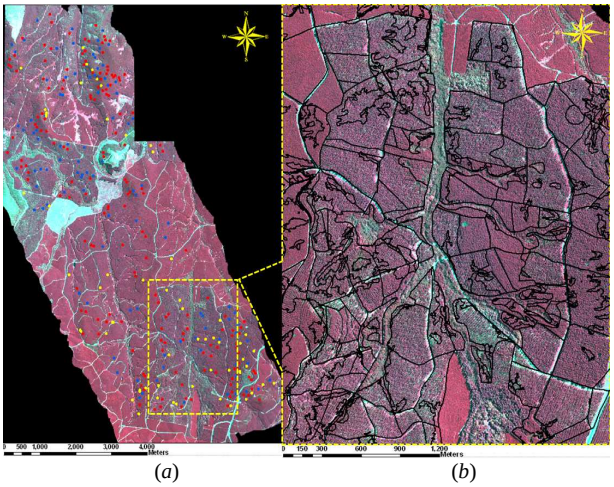

(*a*) (*b*)

Figure 1. (*a*)Study area and the field data (yellow circles) as well as sample plots, training data (red circles) and test data (blue circles) shown on WV-2 false colour image (7, 5 and 3 as red, green and blue); (*b*) the aerial photogrammetric interpretation (API) map

2.2 Remotely Sensed data

An airborne HARRIER 56/G3 fully-integrated sensor with LMS-Q560 laser scanner (Riegl, Austria) collected lidar data in July, 2008 over the study area. The acquisition parameters were set to achieve a pulse rate of 88,000 Hz, 60 cm footprint size and 2 pulses per m^2 with a maximum scan angle of 15°. Following the collection of the lidar data, a 0.5 m resolution DTM was generated by applying a standard triangular irregular networks (TIN) modelling technique. A digital surface model (DSM) with matching pixel resolution was generated by selecting the highest lidar point elevation value per cell. Finally, the DTM was subtracted from the DSM to construct a canopy height model (CHM).

The orthorectified WV-2 multispectral images with 2 m spatial resolution used in this study were acquired on 9 March 2010, which is not the same as the lidar acquisition and field data inventory, as the WV-2 sensor was not yet operational. This time lag could be a potential source of error in the analysis of this data. However, using an aerial photogrammetry interpretation (API) map of the plantation, containing information such as age and thinning conditions for different parts of the plantation and provided by Forests NSW, the collected plots were compared with the content of the WV-2 multispectral image and it was determined that no harvesting or thinning had occurred during this 17 month time lag. Moreover, 17 months plot growth would not considerably affect the plot-level statistics in low rainfall years of 2008 and 2009 (Shamsoddini et al., 2013a). The WV-2 sensor provides 8 multispectral bands including 4 traditional remotely sensed bands of blue, green, red and near infrared (NIR1), and 4 new bands comprising of coastal blue, yellow, red edge and a new near infrared band (NIR2).

2.3 Sampling Design

Training and testing of the prediction models required the collection of some samples over the plantation. To achieve this aim, the irrelevant areas such as Eucalypts patches, bare and grass lands were masked out using the API map. Spatial autocorrelation amongst samples that could potentially violate the assumption of the sample independence should be taken into account prior to the collection of the sample (Congalton and Green, 2009). Semi-variograms are the most common method for determining the minimum distance at which spatial autocorrelation is expected to occur among pixels of remotely sensed data (Hyppänen, 1996; Popescu et al., 2004).

The autocorrelation distance over pine plantation is a function of thinning condition and age of trees (Atkinson and Danson, 1988; Cohen et al., 1990; Mason et al., 2007). Three sites including three age classes were considered along with two extreme thinning conditions, unthinned and second thinning by the random-systematic method. The semi-variograms should be calculated for the optical band which reveals more information of the structure of the plantation (Pascual et al., 2010). According to the findings of Shamsoddini et al. (2013a), green band of WV-2 is relatively highly correlated with the structural parameters of the pine plantation, especially mean height. After determining the required distance for sample collection over the green band and lidar-derived CHM to avoid spatial cross correlation between the samples, a systematic-random sampling was designed to collect the required samples for training and test over different strata. Three different strata including: slope (less than 10°, more than 10° and less than 20°, and more than 30°); thinning condition (unthinned, first thinning and second thinning); and tree age (less than 20 years and more than 20 years) were considered using the API map of the plantation to collect the required samples. The collection of training and test samples was conducted with the following considerations:

- At least 10 random samples for each stratum should be collected.
- At least 50 m distance from irrelevant features such as roads and eucalyptus patches within each stratum.
- A minimum distance of 70 m to 90 m was set between training and test samples to avoid the occurrence of spatial autocorrelation.

The above process led to collection of 171 training samples, and 100 test samples which were collected by the random-systematic sampling process within different strata.

3. METHODOLOGY

Figure 2 shows the methodology which was used in this study. As this figure clearly shows, the methodology of this study comprises four steps including pre-processing, attribute calculation, modelling, and assessment.

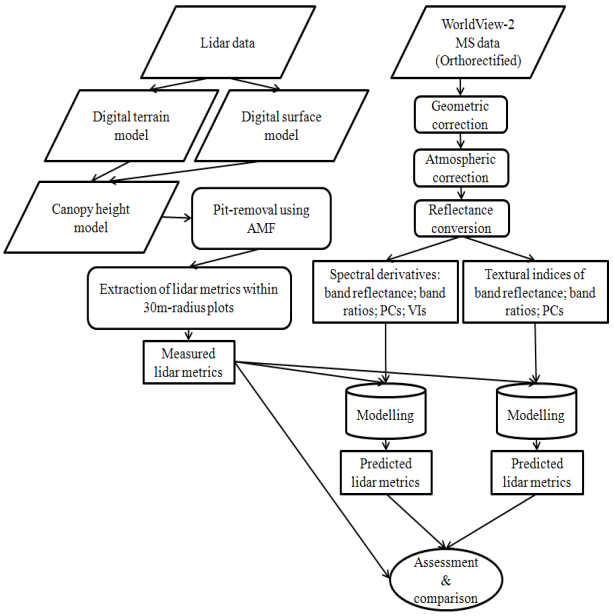

Figure 2. The flow chart of the methodology used in this study

3.1 Pre-processing

The lidar-derived CHM suffers from pit phenomenon which is defined as randomly-distributed pixels whose values are lower than their neighbouring pixels within a crown (Shamsoddini et al., 2013b). Prior to calculation of statistical metrics, it is required to reduce the effect of pits on the CHM (Shamsoddini et al., 2013b). Pit removal was conducted using adaptive mean filter (AMF) with 7×7 window size developed by Shamsoddini et al. (2013b).

The WV-2 multispectral imagery was orthorectified by the data provider (DigitalGlobe) with a horizontal accuracy of 6.8 m which is more than 3 times the spatial resolution of the data. To improve the geo-referencing accuracy, they were referenced to the lidar-derived CHM based on 70 ground identifiable control points identified on the optical image and CHM using a first order polynomial function. The accuracy of the georeferencing was approximately 0.8 m or less than half of a pixel. Dark object subtract method (DOS3) was exploited to atmospherically correct WV-2 data and digital numbers were converted to reflectance values. Moreover, cos (i), which is the incident angle between the sun and a horizontal surface was calculated according to Riano et al. (2003). There was no need for topographic correction as the examination of the relationship between cos (i) and the radiance of each band did not show significant correlation after removal of path radiance.

3.2 Attribute Calculation

10 statistical attributes including mean (*ME*); maximum (*MAX*); variance (*VAR*); standard error of the mean - standard deviation divided by the square root of the number of pixels - (*SEM*); skewness (*SK*); kurtosis (*KU*), and 10^{th}, 30^{th}, 60^{th} and 90^{th} height percentiles were calculated for the collected samples within 30 m radius plots. The reasons for the selection of this plot size were discussed in Shamsoddini et al. (2013a).

The reflectance of individual bands, ratios of band reflectance, and principal components (PCs) were calculated for WV-2 data. In addition, 11 vegetation indices comprising normalized difference vegetation index (NDVI), normalized yellow index (NYI), near infrared NDVI (NIRNDVI), optimized soil-adjusted vegetation index (OSAVI), ratio vegetation index (RVI), yellow NDVI (YNDVI), global environment monitoring index (GEMI), modified simple ratio (MSR), modified chlorophyll absorption in reflectance index2 (MTVI2), transformed SAVI (TSAVI), and weighted difference vegetation index (WDVI) which proved to be useful for pine plantation structure mapping (Shamsoddini, 2012; Shamsoddini et al., 2012; Shamsoddini et al., 2013a) were also calculated. Those indices involving the NIR band were calculated using both NIR1 and NIR2 bands for WV-2. 11 GLCM indices, *mean* (*GME*), *variance* (*GVAR*), *standard deviation* (*ST*), *contrast* (*CON*), *angular second moment* (*ASM*), *entropy* (*ENT*), *homogeneity* (*HOM*), *energy* (*EN*), *correlation* (*COR*), *dissimilarity* (*DISS*), and *maximum probability* (*MP*), were calculated for four window sizes, 3×3, 5×5, 7×7, and 9×9, and for four orientations, 0°, 45°, 90° and 135°.

According to Gao et al. (2000) and Shamsoddini et al. (2013a), bands, band ratios and PCs provide different types of information. For this reason, the textural indices were calculated for bands, band ratios and PCs derived from WV-2 multispectral image. To reduce the number of attributes and increase the efficiency of the feature selection process which is a stepwise method, the absolute value of the Pearson correlation coefficient was calculated for each possible pair of attributes. Then the summation of the absolute value of the correlation coefficient derived for the examination of the relationship between each attribute with the others was calculated. Each pair of attributes whose correlation coefficient was higher than 0.90 was considered to be redundant and the one whose total correlation coefficient was higher than the other was removed.

3.3 Modelling

As mentioned, multiple-linear regression is the common method for modelling lidar metrics using optical data. A stepwise multiple-linear regression was used to model the lidar metrics using textural information and spectral derivatives of WV-2. The conditions, explained in Shamsoddini et al. (2013a), were taken into account to avoid multicollinearity and over-fitting of the models developed using multiple-linear regression. The coefficient of determination (R^2), and standard error of estimation (SEE) were calculated to show the fitness of the regression models derived for predicting lidar metrics. The relative error which was calculated using SEE of each lidar

metric divided by its measured mean value was used to provide comparisons of the accuracy of different lidar metric predictions.

3.4 Assessment and Comparison

After modelling the lidar metrics using WV-2 data, they were assessed to reveal whether the predictions are statistically significant from those derived from the measured lidar data. This was based on a paired-samples t-test to indicate the significance of the difference between measured and predicted lidar metrics. Also this statistical test was applied for comparing the results achieved from spectral and textural attributes.

4. RESULTS AND DISSCUSSION

After deriving the final textural and spectral-based models of WV-2 data, based on lower SEE and higher R^2, they were applied to predict the lidar metrics for the test samples. Figure 3 reveals the results of the lidar metric prediction for 100 test plots. According to figure 3, textural-based models derived from WV-2 data performed better than the spectral-based models for explaining the variability of all lidar metrics. Among lidar metrics, the variation of *VAR*, and *SEM* were explained better than the other lidar metrics (more than 80%). The relative error shown in figure 3(*b*) indicates that the lidar metrics are predicted more accurately using textural-based models compared to the spectral-based models, except for 60^{th} percentile.

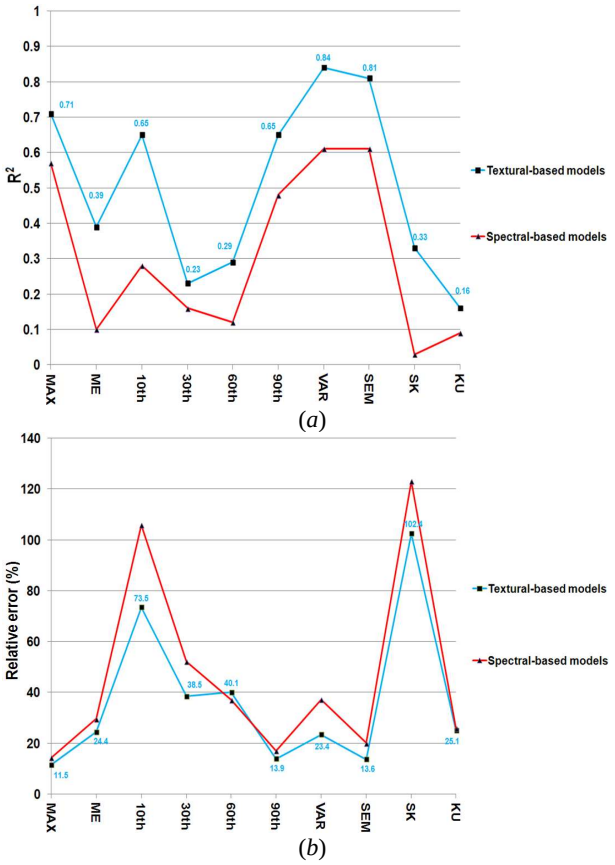

Figure 3. Lidar attributes derived using spectral and textural data of WV-2 multispectral images. (*a*) and (*b*) are for the correlation of determination and relative error respectively derived for the predicted lidar-derived attributes from the test sample plots.

Moreover, the relative error of *MAX*, *SEM*, and 90^{th} percentile is lower than the other metrics (less than 14%). The better prediction of lidar metrics related to the upper parts of the canopy (e.g. *MAX*) compared to those related to the lower parts (e.g. 10^{th} percentile) may be due to the effect of understorey and the presence of pits on the calculation of those metrics for lower parts of canopy.

Paired-samples t-test was applied to examine whether the lidar metrics, predicted by textural-based models, are significantly more accurate than those derived from spectral-based models. Table 1 reveals that the lidar metrics predicted by textural-based models from WV-2 data are significantly more accurate than the spectral-based models, except for 30^{th} and 60^{th} percentiles where there is no significant difference.

Lidar metric	t	Sig. (2-tailed)
MAX	-3.152	0.002*
ME	2.868	0.005*
10^{th} percentile	3.398	0.001*
30^{th} percentile	0.985	0.327
60^{th} percentile	-1.563	0.121
90^{th} percentile	3.651	0.000*
VAR	-4.765	0.000*
SEM	4.438	0.000*
SK	-2.813	0.006*
KU	1.915	0.058

Note: * indicates p-level values which are statistically significant at α of 0.05. Degree of freedom is 99for all cases

Table 1. Paired-samples t-test results for comparison of textural-based and spectral-based models

According to the results, adding spectral attributes to the textural attributes could not significantly improve the accuracy of the lidar metric predictions derived from textural-based models. The paired-samples t-test applied for comparing the mean values of lidar metrics predicted by textural-based models and the measured lidar metrics indicated that there is no significant difference between the two sets of lidar metrics; however, it is necessary to examine the reliability of the predicted lidar metrics for different forest applications such as structural parameter estimation.

The analysis of the spectral derivatives and textural attributes which were selected by stepwise method for the final prediction models provided some useful considerations. For spectral-based models, NIRNDVI, NYI, and TSAVI are more important than the other VIs for predicting lidar metrics. These vegetation indices were also useful for estimating structural parameter of the pine plantation in Shamsoddini et al. (2013a). As table 2 shows the textural indices selected by the models, textural attributes derived from PC6 and PC5 of WV-2 were the most important predictors of the textural-based models. Also, The band ratio of vegetation-insensitive and vegetation sensitive bands especially coastal blue and other WV-2 vegetation-sensitive bands such as green, yellow, and red edge are frequently selected as predictors of the textural-based models of WV-2. According to literature (Gao et al., 2000; Castro et al., 2003, Shamsoddini et al., 2013a), the ratio of the vegetation-insensitive and sensitive bands can perform as efficient indicators for vegetation studies since the effects of phenomena such as atmosphere, shadow and, background are reduced in the ratio output.

Regarding the textural indices, *correlation* and *contrast* were selected as predictors significantly more than other GLCM indices extracted from WV-2. Finally, no window size was

selected as being superior for calculating GLCM attributes, since GLCM attributes are affected by the window size in different ways (Kayitakire et al., 2006). Also, according to table 2, no window orientation was identified as the suitable for extracting GLCM attributes. This can be mainly due to there being no dominant tree row in the pine plantation, especially in the unthinned and second thinning areas, according to the visual inspection of WV-2 data.

Lidar metric	Predictors (WV-2)
MAX	CON0w3b6; GVAR90w9P5; COR135w5b1; MP45w9b2; COR90w9b6-8
ME	COR45w3b1-4; COR90w3b2-3; COR90w7b3-6; GME45w3P3; COR90w3P5; CON45w3b4
10^{th} percentile	COR45w7P1; COR90w9P3; COR90w9b3-4; COR135w7b7-8; MP45w9b2; CON90w3P1; COR90w3P5
30^{th} percentile	COR45w3b2; DISS90w5P6; DISS90w3b1-5; COR0w7b3-4; COR0w7b7; CON90w9b6-7
60^{th} percentile	COR45w3b1-4; CON0w3b6; COR90w3b6-8; GVAR90w9b2-4; COR90w3b5; DISS135w9P6; COR0w3b1-2; GME0w9P4; CON90w9b6-7
90^{th} percentile	CON0w3b6; GME45w3P6; GVAR0w9b4-5; COR0w3b6-8; GVAR90w9P5
VAR	COR90w9P4; GME45w3P6; CON0w3b6; COR0w5P4; DISS90w3P7; GVAR90w9b7-8; CON0w3b3-5; COR90w9b6-8
SEM	CON0w3b6; GME45w3P6; GVAR90w9P5; MP45w9b2; COR135w5P5; COR0w3b2-5; CON0w3b3-4
SK	COR45w3b1-3; DISS90w5P6; GME45w3b1-8; COR0w9b6-7; COR90w3b5; GVAR90w9b1-4; DISS90w3b6-8
KU	GME45w3P6; ST0w9b3-4; COR45w3P5; CON0w3b3-4

Note: in this table the code to the GLCM attribute is shown by xx dx wx yx, where xx presents the abbreviation name of attributes. dx and wx show the orientation and window size, respectively and yx represents PC number if y is P; otherwise it shows the number of band or band ratio.

Table 2. Textural indices selected by the models developed for predicting each lidar metrics

5. CONCLUSION

The utility of WV-2 multispectral image for predicting lidar metrics over a *Pinus radiata* plantation at plot level was investigated. It was indicated that the WV-2 data including spectral and textural data are useful for lidar metric prediction. The textural-based models result in significantly more accurate predictions of lidar metrics compared to those derived from spectral-based models. Adding spectral derivatives to the textural attributes of WV-2 did not improve the accuracy of the lidar metric predictions derived from textural-based models. It was demonstrated that PCs can perform much better than the other spectral information of WV-2 for predicting lidar metrics. Among different textural indices, *correlation*, *mean*, and *contrast* are more useful than the others. It is suggested that the prediction accuracy of higher percentile lidar metrics, e.g. 90^{th} and *MAX*, are better than those pertaining to the lower percentiles, e.g. 10^{th}, 30^{th}, and *ME*. Although, the statistical examination of the results showed no difference between measured and predicted lidar metrics, investigation of the reliability of the predicted lidar metrics, especially for estimating different structural parameters should be investigated further.

Acknowledgement

Lidar-derived data utilized in this study was kindly supplied by Dr. Christine Stone from the New South Wales Department of Industry and Investment (IINSW) and Forests NSW (FNSW), with partial sponsorship from the Forest and Wood Products Australia (FWPA). Moreover, the authors are grateful to DigitalGlobe for providing WorldView-2 multispectral image.

Reference

Atkinson, P. M. & Danson, F. M., 1988. Spatial Resolution for Remote Sensing of Forest Plantations. In*:* Geoscience and Remote Sensing Symposium, IGARSS '88, 1, pp. 221-223.

Castro, K. L., Sanchez-Azofeifa, G. A., & Rivard, B., 2003. Monitoring secondary tropical forests using space-borne data: Implications for Central America. *International Journal of Remote Sensing*, 24, pp. 1853-1894.

Chen, G. & Hay, G. J., 2011. An airborne lidar sampling strategy to model forest canopy height from Quickbird imagery and GEOBIA. *Remote Sensing of Environment*, 115, pp. 1532-1542.

Chen, X., Liu, S., Zhu, Z., Vogelmann, J., Li, Z., & Ohlen, D., 2011. Estimating aboveground forest biomass carbon and fire consumption in the U.S. Utah High Plateaus using data from the Forest Inventory and Analysis Program, Landsat, and LANDFIRE. *Ecological Indicators*, 11, pp. 140-148.

Congalton, R. G., & Green, K, 2009. *Assessing the accuracy of remotely sensed data: principles and practices* (second ed.). CRC Press, Boca Raton.

Cohen, W. B., Spies, T. A., & Bradshaw, G. A., 1990. Semivariograms of digital imagery for analysis of conifer canopy structure. *Remote Sensing of Environment*, 34, pp. 167-178.

Dean, T. J., Cao, Q. V., Roberts, S. D., & Evans, D. L., 2009. Measuring heights to crown base and crown median with LiDAR in a mature, even-aged loblolly pine stand. *Forest Ecology and Management*, 257, pp. 126-133.

Donoghue, D. N. M. & Watt, P. J., 2006. Using LiDAR to compare forest height estimates from IKONOS and Landsat ETM+ data in Sitka spruce plantation forests. *International Journal of Remote Sensing*, 27, pp. 2161-2175.

Erdody, T. L., & Moskal, L. M., 2010. Fusion of LiDAR and imagery for estimating forest canopy fuels. *Remote Sensing of Environment*, 114, pp. 725-737.

Gao, X., Huete, A. R., Ni, W., & Miura, T., 2000. Optical-biophysical relationships of vegetation spectra without background contamination. *Remote Sensing of Environment*, 74, pp. 609-620.

Hilker, T., Wulder, M. A. & Coops, N. C., 2008. Update of forest inventory data with lidar and high spatial resolution satellite imagery. *Canadian Journal of Remote Sensing*, 34, pp. 5-12.

Hsieh, W. W., 2009. *Machine learning methods in the environmental sciences*. Cambridge University Press, Cambridge.

Hyde, P., Dubayah, R., Walker, W., Blair, J. B., Hofton, M., & Hunsaker, C., 2006. Mapping forest structure for wildlife habitat analysis using multi-sensor (LiDAR, SAR/InSAR, ETM+, Quickbird) synergy. *Remote Sensing of Environment*, 102, pp. 63-73.

Hyppänen, H., 1996. Spatial autocorrelation and optimal spatial resolution of optical remote sensing data in boreal forest environment. *International Journal of Remote Sensing*, 17, pp. 3441-3452.

Hyyppä, J., Hyyppä, H., Inkinen, M., Engdahl, M., Linko, S., & Zhu, Y.-H., 2000. Accuracy comparison of various remote sensing data sources in the retrieval of forest stand attributes. *Forest Ecology and Management*, 128, pp.109-120.

Hyyppä, J., Hyyppä, H., Leckie, D., Gougeon, F., Yu, X., & Maltamo, M., 2008. Review of methods of small-footprint airborne laser scanning for extracting forest inventory data in boreal forests. *International Journal of Remote Sensing*, 29, pp. 1339 - 1366.

Hyyppä, J., Kelle, O., Lehikoinen, M., & Inkinen, M., 2001. A segmentation-based method to retrieve stem volume estimates from 3-D tree height models produced by laser scanners. *IEEE Transactions on Geoscience and Remote Sensing*, 39, pp. 969-975.

Jinha, J., & Crawford, M. M., 2012. Extraction of features from LIDAR waveform data for characterizing forest structure. *IEEE Geoscience and Remote Sensing Letters*, 9, pp. 492-496.

Kayitakire, F., Hamel, C., & Defourny, P., 2006. Retrieving forest structure variables based on image texture analysis and IKONOS-2 imagery. *Remote Sensing of Environment*, 102, pp.390-401.

Lefsky, M. A., Cohen, W. B., & Spies, T. A., 2001. An evaluation of alternate remote sensing products for forest inventory, monitoring, and mapping of Douglas-fir forests in western Oregon. *Canadian Journal of Forest Research*, 31, pp. 78-87.

Le Toan, T., Shaun, Q., Woodward, I., Lomas, M., Delbart, N., & Picard, G., 2004. Relating RADAR remote sensing of biomass to modelling of forest carbon budgets. *Climate Change*, 67, pp. 379-402.

Lim, K., Treitz, P., Wulder, M., St-Onge, B., & Flood, M., 2003. LiDAR remote sensing of forest structure. *Progress in Physical Geography*, 27, pp. 88-106.

Mason, W. L., Connolly, T., Pommerening, A., & Edwards, C., 2007. Spatial structure of semi-natural and plantation stands of Scots pine (Pinus sylvestris L.) in northern Scotland. *Forestry*, 80, pp. 567-586.

Means, J. E., Acker, S. A., Harding, D. J., Blair, J. B., Lefsky, M. A., Cohen, W. B., Harmon, M. E. & McKee, W. A., 1999. Use of large-footprint scanning airborne lidar to estimate forest stand characteristics in the Western Cascades of Oregon. *Remote Sensing of Environment*, 67, pp. 298-308.

Pascual, C., García-Abril, A., Cohen, W. B., & Martín-Fernández, S., 2010. Relationship between LiDAR-derived forest canopy height and Landsat images. *International Journal of Remote Sensing*, 31, pp. 1261-1280.

Popescu, S. C., Wynne, R. H., & Nelson, R. F., 2002. Estimating plot-level tree heights with lidar: local filtering with a canopy-height based variable window size. *Computers and Electronics in Agriculture*, 37, pp. 71-95.

Popescu, S., C., Wynne, R., H. & Scrivani, J., A., 2004, Fusion of small-footprint lidar and multispectral data to estimate plot-level volume and biomass in deciduous and pine forests in Virginia, USA. *Forest Science*, 50, pp. 551-565.

Riano, D., Chuvieco, E., Salas, J., & Aguado, I., 2003. Assessment of different topographic corrections in Landsat-TM data for mapping vegetation types. *IEEE Transactions on Geoscience and Remote Sensing*, 41, pp. 1056-1061.

Sexton, J. O., Bax, T., Siqueira, P., Swenson, J. J. & Hensley, S., 2009. A comparison of lidar, radar, and field measurements of canopy height in pine and hardwood forests of southeastern North America. *Forest Ecology and Management*, 257, pp. 1136-1147.

Shamsoddini, A., 2012. Radar backscatter and optical textural indices fusion for pine plantation structure mapping. In: ISPRS Annals of the Photogrammetry, Remote Sensing and Spatial Information Sciences, Melbourne, I-7, pp. 309-314.

Shamsoddini, A., Trinder, J. C., & Turner, R., 2012. SPOT-5 multispectral image for pine plantation structure mapping. In: ACRSC2012 proceeding, Thailand, pp. 1-10.

Shamsoddini, A., Trinder, J. C., & Turner, R., 2013a. Pine plantation structure mapping using WorldView-2 multispectral image. *International Journal of Remote Sensing*, 34, pp. 3986-4007.

Shamsoddini, A., Turner, R. & Trinder, J. C., 2013b. Improving lidar-based forest structure mapping with crown-level pit removal. *Journal of Spatial Science*, 58, pp. 29-51.

Shanmugam, P., Ahn, Y.-H., & Sanjeevi, S., 2006. A comparison of the classification of wetland characteristics by linear spectral mixture modelling and traditional hard classifiers on multispectral remotely sensed imagery in southern India. *Ecological Modelling*, 194, pp. 379-394.

Smart, L. S., Swenson, J. J., Christensen, N. L., & Sexton, J. O., 2012. Three-dimensional characterization of pine forest type and red-cockaded woodpecker habitat by small-footprint, discrete-return lidar. *Forest Ecology and Management*, 281, pp. 100-110.

Wulder, M. A., & Seemann, D., 2003. Forest inventory height update through the integration of lidar data with segmented Landsat imagery. *Canadian Journal of Remote Sensing*, 29, pp.536-543.

Zimble, D. A., Evans, D. L., Carlson, G. C., Parker, R. C., Grado, S. C., & Gerard, P. D., 2003. Characterizing vertical forest structure using small-footprint airborne LiDAR. *Remote Sensing of Environment*, 87, pp. 171-182.